OFDMA-CDM Performance Enhancement by Combining H-ARQ and Interference Cancellation

Alexander Arkhipov, Ronald Raulefs, and Michael Schnell, *Senior Member, IEEE*

***Abstract*—In this paper, superimposed packet allocation for orthogonal frequency-division multiple-access code-division multiplexing (OFDMA-CDM) is presented, where each transmitted packet is associated with one spreading code. An iterative algorithm which is a combination of parallel interference cancellation and hybrid automatic repeat request (H-ARQ) based on soft value combining (SVC) is proposed, and its performance is studied and compared with other existing H-ARQ schemes. The proposed algorithm exploits the reliability information of erroneously received copies of the same data packet to improve the performance of interference cancellation. The interference of correctly received packets is ideally reconstructed and subtracted. Thus, the overall system performance improves iteratively. As a result, the proposed algorithm outperforms conventional H-ARQ based on SVC, as well as H-ARQ based on maximum ratio combining.**

***Index Terms*—Automatic repeat request, interference suppression.**

I. Introduction

WIRELESS systems of the next-generation must provide high spectral efficiency, offer high data rates and high user capacity. The multicarrier multiple-access scheme realized by a combination of orthogonal frequency-division multiple-access (OFDMA) [1] with code-division multiplexing (CDM) attracts significant interest because of its robustness to multipath propagation and its high spectral efficiency [2]. In OFDMA-CDM, each transmitted symbol is spread over several subcarriers and the CDM component is used to transmit several symbols in parallel on the same subcarriers. The OFDMA component assures orthogonal user discrimination by assigning different users separate sets of subcarriers. Thus, multiple-access interference is avoided. Nevertheless, self-interference (SI) occurs in frequency-selective fading channels due to the loss of orthogonality of spreading codes. In order to cope with SI, a soft parallel interference cancellation (PIC) scheme [2], [3] is used as an efficient data detection and decoding technique.

In [2], an OFDMA-CDM system with convolutional codes is compared with conventional OFDMA with turbo codes [4]. The results, obtained for independent Rayleigh-fading, show that OFDMA-CDM with soft PIC can outperform OFDMA with turbo codes.

Manuscript received April 1, 2005; revised October 1, 2005. This paper was supported in part by the European Commission within FP6 under Contract IST-2002-507039 carried out in the framework of the 4MORE (4G MC-CDMA Multiple Antenna System on Chip for Radio Enhancements) Project. This paper was presented in part at the IEEE 61st Semiannual Vehicular Technology Conference, Stockholm, Sweden, 2005

The authors are with the German Aerospace Center (DLR), Institute of Communications and Navigation, 82234 Wessling, Germany (e-mail: alexander.arkhipov@dlr.de; Ronald.Raulefs@dlr.de; Michael.Schnell@dlr.de).

Digital Object Identifier 10.1109/JSAC.2005.864004

Iterative (turbo) soft interference cancellation is described in [5]. In this algorithm, the extrinsic information is extracted from the detection and decoding stages and then used as *a priori* information in the next iteration, just as in turbo decoding.

To achieve error-free transmission some error control techniques are adopted. Hybrid-automatic repeat request (H-ARQ) is one of the most familiar schemes. Several types of H-ARQ [6] can be distinguished, namely, H-ARQ with incremental redundancy (IR) [7] and H-ARQ with Chase combining [8]. In Chase combining, the same data packet is transmitted upon a repeat request, and the soft decision statistics from all retransmissions are coherently combined either at symbol or at bit level. For symbol level combining, H-ARQ based on maximum ratio combining (MRC) is used, since MRC provides the best signal-to-noise ratio (SNR). For soft value combining (SVC), the combination of an arbitrary number of soft decoded packets can be considered as an additional repetition code. The IR scheme typically does not retransmit the original transmission packet; the additionally transmitted packets carry redundancy information, i.e., parity bits for error correction. These additional redundancy bits are combined with the previously received bits, decreasing the effective code rate after each additional transmission.

A high-speed link based on multicarrier code-division multiple access (MC-CDMA) combined with efficient multilevel modulation, linear detection techniques, and H-ARQ has been proposed in [9]. It has been shown that the proposed transmission system with 8-PSK and 16-QAM modulation cardinality suffers from a higher level of SI, and the achievable throughput cannot be improved sufficiently unless a more powerful channel code is used.

Performance comparisons of H-ARQ with IR and Chase combining have been carried out in [10]–[12]. It has been shown that, despite the superiority of IR over Chase combining, the performance of IR and Chase combining is almost identical in slowly changing fading channels if adaptive modulation and coding is used. Furthermore, the performance of IR and Chase combining is the same at high SNR, at a working point where the packet error rate does not exceed 5%. Different algorithms have been proposed in order to improve the performance of H-ARQ with Chase combining. Examples include: additional bit interleaving [13], symbol interleaving [14] between retransmissions, and constellation rearrangement [15].

In the past, research focused solely on optimizing each layer of the OSI layer scheme. Recently [16], the focus broadened to overcome existing limits more easily by jointly exploiting resources in the physical as well as in the data link layer. In [10] for example, the authors used H-ARQ as a possible method to increase the potential diversity in their proposal for wire-

less systems. In this contribution, we combine a soft IC scheme on the physical layer with an H-ARQ scheme on the data link layer to increase and exploit the potential diversity jointly by the channel code and by the interference cancellation scheme. This cross-layer approach allows to improve the performance, as well as to decrease latency. Latency can be reduced by minimizing retransmissions of not perfectly decoded data symbols, which is an important issue in CDMA-based systems applying H-ARQ based on MRC. As all chips of a data symbols need to be retransmitted, the overall throughput decreases, thus, increasing latency. Combining soft interference cancellation and H-ARQ achieves both better performance and reduced latency.

We propose to associate each transmitted packet with one spreading code and develop an efficient algorithm that is a combination of H-ARQ based on SVC and PIC. In the proposed algorithm, reliability information of erroneously received copies of the same data packet is used in order to improve the quality of interference cancellation. As shown later, this approach significantly improves the system throughput both at the working point and for lower SNR. It is worth noting that such a scheme can be combined with H-ARQ using IR, but such a combination is out of the scope of this work.

Moreover, we investigate the performance of the proposed algorithm, study the advantages of superimposed packet allocation within a frame and underline the difference between H-ARQ based on SVC and H-ARQ based on MRC. Applying different types of H-ARQ, we compare the performance of OFDMA-CDM and conventional OFDMA.

The remainder of this paper is organized as follows: Section II contains the general description of the transmission structure, while Section III describes the advanced parallel interference cancellation (APIC) scheme, which is a combination of H-ARQ based on SVC and a soft PIC scheme. The simulation results are given in Section IV. Finally, Section V concludes the work.

II. OFDMA-CDM Transmission Scheme

In an OFDMA-CDM system, different users utilize separate sets of subcarriers for data transmission. Thus, all users are orthogonal to each other and this allows to consider the data transmission of a single user in the following. For convenience, indices which distinguish different users are omitted.

In Fig. 1, an OFDMA-CDM transmitter is shown which is able to transmit L packets of equal size simultaneously by applying spreading codes of length L within the CDM component. At the end of each packet, cyclic redundancy check (CRC) bits are appended. The packet is decoded at the receiver and is considered error-free if the CRC passes. In this case, a positive acknowledgment (ACK) is generated and sent back to the transmitter. Otherwise, a negative acknowledgment (NACK) is sent back and the transmission of the erroneously decoded packet is repeated. It is assumed that ACK from the receiver to the transmitter are error-free and buffer overflows occur neither at the transmitter nor at the receiver. The maximum allowed number of transmissions is limited to N_{tr}. If the packet cannot be decoded in N_{tr} transmissions, the receiver discards the packet. In the following, for each packet l, $l = 1, \ldots, L$, the total number

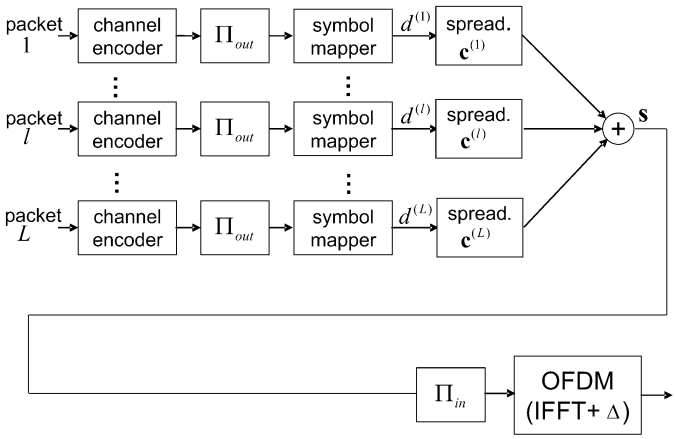

Fig. 1. Proposed OFDMA-CDM transmitter.

of occurred transmissions is defined as $M_l \leq N_{\mathrm{tr}}$. At the physical layer, L packets are simultaneously transmitted within one frame, which consists of N_{fr} OFDMA-CDM symbols.

After channel encoding and outer interleaving Π_{out} the coded bits $b^{(l)}$, $l = 1, \ldots, L$, are symbol mapped, yielding complex-valued data symbols. The outer interleaving is constructed in such a way that it performs independent random interleaving between the retransmissions, which allows the system to exploit time and frequency diversity between retransmissions.

Data symbols from different packets are transmitted in groups of L data symbols. In each group, only one data symbol from each packet is transmitted. The number of groups transmitted within one OFDMA-CDM symbol is denoted as Q, in the sequel. Thus, Q symbols of each packet are transmitted within one OFDMA-CDM symbol, using LQ subcarriers. The intention of such a group allocation can be explained as follows. It allows to increase the size of a transmitted packet because each packet occupies LQ chips within one OFDMA-CDM symbol. Therefore, additional frequency diversity can be achieved [1]. Additionally, such a group allocation allows to keep the spreading length relatively small, which decreases the complexity of interference cancellation. Assume that vector $\mathbf{d} = (d^{(1)}, d^{(2)}, \ldots, d^{(L)})^T$ represents the data symbols of one group. The sequence $\mathbf{s}$ represents spread data symbols of one group and is written as

$$\mathbf{s} = \mathbf{C}_L \mathbf{d} \tag{1}$$

where a Walsh–Hadamard (WH) transformation [17]

$$\mathbf{C}_L = \begin{pmatrix} \mathbf{C}_{L/2} & \mathbf{C}_{L/2} \\ \mathbf{C}_{L/2} & -\mathbf{C}_{L/2,} \end{pmatrix} \forall L = 2^{\kappa}, \kappa \geqslant 1, \mathbf{C}_1 = 1 \tag{2}$$

is applied to perform spreading. The resulting L columns $\mathbf{c}^{(l)}$, $l = 1, \ldots, L$, of matrix $\mathbf{C}_L$ represent the orthogonal spreading codes. This transformation allows one orthogonal WH spreading code $\mathbf{c}^{(l)}$ to be associated with each transmitted packet l, $l = 1, \ldots, L$.

The resulting sequence $\mathbf{s}$ is transmitted within one OFDMA-CDM symbol. After inner frequency interleaving Π_{in}, the elements of $\mathbf{s}$ are transmitted on separate subcarriers by performing an OFDM modulation. A guard interval $\triangle$, which is larger than the maximum delay of the transmission channel is added. The guard interval $\triangle$ avoids intersymbol interference with the preceding OFDMA-CDM symbol.

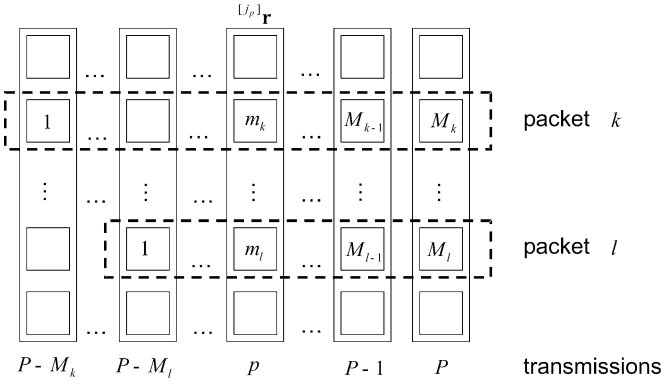

Fig. 2. The content of the buffer of received values.

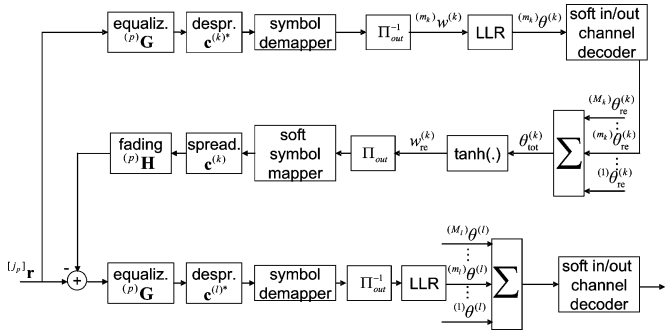

Fig. 3. Proposed interference cancellation scheme with re-encoded values combining.

In OFDMA-CDM systems, each subcarrier is exclusively used by a single user, and no multiple-access interference occurs. The total number of subcarriers is $N_c = K_{\max}LQ$, where $K_{\max}$ is the maximum number of simultaneously active users, which use a different set of subcarriers. Therefore, the OFDMA-CDM scheme can be applied in the downlink, as well as in the uplink. The OFDMA-CDM symbols are transmitted over a frequency-selective mobile radio channel, where the orthogonality of the spreading codes is lost. At the receiver, an inverse OFDM operation is performed. After frequency deinterleaving, the received sequence $\mathbf{r}$ in the frequency domain is given by

$$\mathbf{r} = \mathbf{H}\mathbf{s} + \mathbf{n} \tag{3}$$

where $\mathbf{H} = diag(H_1, \ldots, H_L,)$ is a diagonal matrix, whose complex-valued diagonal elements represent the fading on the subcarriers on which $\mathbf{s}$ has been transmitted. Additive white Gaussian noise with variance $\sigma^2/2$ per dimension is denoted by the L-dimensional vector $\mathbf{n}$.

The received vector $\mathbf{r}$ is passed to the APIC block, where the algorithm is applied, as described in the next section. The APIC generates an "ACK" or "NACK" for each received packet.

III. Advanced Parallel Interference Cancellation Scheme

A. Re-encoded Values Combining

The received vector $\mathbf{r}$ and matrix $\mathbf{H}$ are saved into a buffer of received values and fading values, respectively. Without loss of generality, we assume that $P-1$ vectors are already stored in each buffer. Thus, the received vector $\mathbf{r}$ and $\mathbf{H}$ represent the Pth elements in the buffers. In the following, we introduce the subscript $p = 1, \ldots, P$, which denotes the index number of the elements in the buffers.

In Fig. 2, the matrix-like structure demonstrates the content of the buffer of received values, where the columns denote the received vectors and the rows define the transmitted packets.

The proposed algorithm is performed in multiple iterations. In each iteration, up to L packets can be decoded. In the following, index j_p, $j_p = 1, \ldots, L$, denotes the number of packets, whose contributions are ideally subtracted from the received vector $\mathbf{r}$ resulting in ${}^{[j_p]}\mathbf{r}$. The notation ${}^{[j_p]}\mathbf{r}$ refers to the vector received after the pth transmission from which the interference of j_p other packets has been removed.

For convenience, we introduce the decision status values ${}^{(p)}\mathrm{DS}^{(l)} \in \{\mathrm{true}, \mathrm{false}\}$, $l = 1, \ldots, L$, $p = 1, \ldots, P$. The expression "${}^{(p)}\mathrm{DS}^{(l)} = \mathrm{true}$" means that packet l has been successfully decoded and its contribution is ideally removed from ${}^{[j_p]}\mathbf{r}$.

We illustrate the improved interference cancellation scheme by considering the transmission p in Fig. 2. The packet l will be decoded by removing the interference of packets $k = 1, \ldots, L$, $k \neq l$. The scheme for the interference subtraction is depicted in Fig. 3. In this algorithm, the data symbols of the packets $k = 1, \ldots, L$, $k \neq l$, ${}^{(p)}DS^{(k)} = \mathrm{false}$, are detected and decoded. Finally, the interference contribution of the m_kth transmission of packet k is reconstructed and subtracted from the received signal ${}^{[j_p]}\mathbf{r}$. The data symbols of the m_lth transmission of packet l are detected in the lowest path of Fig. 3.

A minimum mean-square error (MMSE) detector is used to combat the phase and amplitude distortions caused by multipath propagation on the subcarriers. The matrix of equalization coefficients of the transmission p is denoted as ${}^{(p)}\mathbf{G}$, whose diagonal elements ${}^{(p)}G_i$, $i = 1, \ldots, L$ are given by

$${}^{(p)}G_i = \frac{{}^{(p)}H_i^*}{|{}^{(p)}H_i|^2 + \sigma^2}. \tag{4}$$

The output of the outer deinterleaver Π_{out}^{-1} delivers a soft estimate ${}^{(m_k)}w^{(k)}$ for the transmitted code bit $b^{(k)}$ within the m_kth transmission of packet k. The log-likelihood ratio (LLR) of the transmitted bit $b^{(k)}$ given ${}^{(m_k)}w^{(k)}$ is [17]

$${}^{(m_k)}\theta^{(k)} = \ln\left(\frac{P(b^{(k)} = +1|{}^{(m_k)}w^{(k)})}{P(b^{(k)} = -1|{}^{(m_k)}w^{(k)})}\right) \tag{5}$$

and assumes values in the interval $(-\infty, +\infty)$. For OFDMA-CDM with an MMSE detector the LLR in (5) can be represented as [2]

$${}^{(m_k)}\theta^{(k)} \approx \frac{4}{\sigma^2 L}{}^{(m_k)}w^{(k)} \sum_{i=1}^{L} |{}^{(p)}H_i| \tag{6}$$

where ${}^{(p)}H_i$, $i = 1, \ldots, L$, describes the fading on the L subcarriers on which bit $b^{(k)}$ has been transmitted.

The LLR ${}^{(m_k)}\theta_{\mathrm{re}}^{(k)}$ of a re-encoded bit is defined as [2], [3]

$${}^{(m_k)}\theta_{\mathrm{re}}^{(k)} = \ln\left(\frac{P\{b^{(k)} = +1|{}^{(m_k)}\mathbf{w}^{(k)}\}}{P\{b^{(k)} = -1|{}^{(m_k)}\mathbf{w}^{(k)}\}}\right) \tag{7}$$

where the vector ${}^{(m_k)}\mathbf{w}^{(k)}$ represents the sequence of all estimates within the m_kth transmission of packet k. For simplicity, we have omitted an index in the notation ${}^{(m_k)}w^{(k)}$ which indicates a certain soft estimate within the vector ${}^{(m_k)}\mathbf{w}^{(k)}$.

According to (7), the LLR ${}^{(m_k)}\theta_{\mathrm{re}}^{(k)}$ which reflects the reliability of the re-encoded bit is calculated taking into account all soft estimates ${}^{(m_k)}\mathbf{w}^{(k)}$ of packet k.

In the following, soft decided values ${}^{(m_k)}\mathbf{w}^{(k)}, 1, \ldots, M_k$, of the M_k available transmissions of packet k are exploited in order to improve the estimate of the re-encoded values. In comparison to (7), we define the overall LLR value as

$$\theta_{\mathrm{tot}}^{(k)} = \ln\left(\frac{P\{b^{(k)}=+1|{}^{(1)}\mathbf{w}^{(k)},\ldots,{}^{(M_k)}\mathbf{w}^{(k)}\}}{P\{b^{(k)}=-1|{}^{(1)}\mathbf{w}^{(k)},\ldots,{}^{(M_k)}\mathbf{w}^{(k)}\}}\right). \quad (8)$$

The soft values ${}^{(m_k)}\mathbf{w}^{(k)}$ can be assumed conditionally independent given $b^{(k)}$, since the measurement errors introduced by the multipath channel and noise are assumed independent. This assumption can be made, if random outer interleaving between different transmissions is applied. In this case, (8) can be further developed as

$$\begin{aligned}\theta_{\mathrm{tot}}^{(k)} &= \ln\left(\frac{P\{b^{(k)}=+1|{}^{(1)}\mathbf{w}^{(k)},\ldots,{}^{(M_k)}\mathbf{w}^{(k)}\}}{P\{b^{(k)}=-1|{}^{(1)}\mathbf{w}^{(k)},\ldots,{}^{(M_k)}\mathbf{w}^{(k)}\}}\right)\\ &= \ln\left(\frac{P\{b^{(k)}=+1\}}{P\{b^{(k)}=-1\}}\right)\\ &\quad+\sum_{u=1}^{M_k}\ln\left(\frac{P\{{}^{(u)}\mathbf{w}^{(k)}|b^{(k)}=+1\}}{P\{{}^{(u)}\mathbf{w}^{(k)}|b^{(k)}=-1\}}\right)=\sum_{u=1}^{M_k}{}^{(u)}\theta_{\mathrm{re}}^{(k)}. \quad (9)\end{aligned}$$

We assume that both realizations of $b^{(k)}$ are equally probable and, thus

$$\ln\left(\frac{P\{b^{(k)}=+1\}}{P\{b^{(k)}=-1\}}\right)=0. \quad (10)$$

To transfer the LLR value $\theta_{\mathrm{tot}}^{(k)}$ into the bit domain, the average value of $b^{(k)}$, or the so-called "soft bit" [18] is used

$$\begin{aligned}w_{\mathrm{re}}^{(k)} &= E\{b^{(k)}|{}^{(1)}\mathbf{w}^{(k)},\ldots,{}^{(M_k)}\mathbf{w}^{(k)}\}\\ &= (+1)P\{b^{(k)}=+1|{}^{(1)}\mathbf{w}^{(k)},\ldots,{}^{(M_k)}\mathbf{w}^{(k)}\}\\ &\quad+(-1)P\{b^{(k)}=-1|{}^{(1)}\mathbf{w}^{(k)},\ldots,{}^{(M_k)}\mathbf{w}^{(k)}\}. \quad (11)\end{aligned}$$

With (8), the conditional probabilities required in (11) can be written as

$$P\{b^{(k)}=+1|{}^{(1)}\mathbf{w}^{(k)},\ldots,{}^{(M_k)}\mathbf{w}^{(k)}\}=\frac{e^{\theta_{\mathrm{tot}}^{(k)}}}{1+e^{\theta_{\mathrm{tot}}^{(k)}}} \quad (12)$$

and

$$P\{b^{(k)}=-1|{}^{(1)}\mathbf{w}^{(k)},\ldots,{}^{(M_k)}\mathbf{w}^{(k)}\}=\frac{1}{1+e^{\theta_{\mathrm{tot}}^{(k)}}}. \quad (13)$$

Thus, with (12) and (13) the soft bit $w_{\mathrm{re}}^{(k)}$ can be defined as

$$w_{\mathrm{re}}^{(k)}=\frac{e^{\theta_{\mathrm{tot}}^{(k)}/2}-e^{-\theta_{\mathrm{tot}}^{(k)}/2}}{e^{\theta_{\mathrm{tot}}^{(k)}/2}+e^{-\theta_{\mathrm{tot}}^{(k)}/2}}=\tanh\left(\frac{\theta_{\mathrm{tot}}^{(k)}}{2}\right). \quad (14)$$

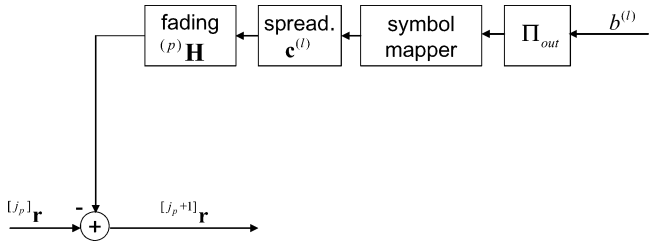

Fig. 4. Ideal interference reconstruction and subtraction.

The soft bit $w_{\mathrm{re}}^{(k)}$ assumes values in the interval $[-1, 1]$. After reinterleaving, the soft bits are modulated such that the reliability information is maintained in the obtained complex-valued data symbols. The obtained soft data symbols are spread, weighted with the channel coefficients and subtracted from the received vector ${}^{[j_p]}\mathbf{r}$.

The summation of re-encoded values obtained in each retransmission according to (9) increases the absolute value of $\theta_{\mathrm{tot}}^{(k)}$, and thus, the feedback loop uses the more reliable estimates of transmitted bits and avoids error propagation.

After interference cancellation of all interfering packets, the data symbols of packet l are detected by applying a single-user detection technique. In contrast to (4), the equalizer coefficients are adopted to the quasi-SI free case and MRC with equalization coefficients given by ${}^{(p)}G_i = {}^{(p)}H_i{}^*$ is used.

The output of the OFDMA-CDM demodulator delivers a complex-valued vector of the symbols of packet l. The received symbols are demapped, and the obtained bits are deinterleaved. Similar to (6), the reliability estimator delivers the LLR values ${}^{(m_l)}\theta^{(l)}$. Since in all transmissions of packet l, copies of the same data are sent, the obtained LLR values are combined to improve the performance of the H-ARQ scheme.

B. H-ARQ Based on SVC

SVC combines several repeated packets encoded with a code rate R [8]. The output of a soft value combiner delivers a value $\sum_{u=1}^{M_l}{}^{(u)}\theta^{(l)}$ for each code bit. The values at the output of a soft value combiner represent the data of packet l encoded with a more powerful error-correcting code of rate R/M_l.

C. Ideal Interference Cancellation

Assume that the CRC verifies an error-free transmission of packet l. In this case, the soft bit is equal to $w_{\mathrm{re}}^{(l)}=1$ if $b^{(l)}=1$ is transmitted or $w_{\mathrm{re}}^{(l)}=-1$, otherwise. Fig. 4 illustrates the obtained simplified interference cancellation scheme. The soft bits $w_{\mathrm{re}}^{(k)}$ or equivalently the correctly decided code bits $b^{(l)}$ within packet l are interleaved and at the output of the symbol mapper the complex-valued data symbols are obtained. The data symbols are spread and the obtained chips are weighted with the appropriate fading coefficients. Then, the reconstructed interference is subtracted from the received vector ${}^{[j_p]}\mathbf{r}$. Finally, the obtained vector ${}^{[j_p+1]}\mathbf{r}$ updates the value ${}^{[j_p]}\mathbf{r}$ in the buffer of the received values.

Proposed Algorithm

```
Algorthm 1. Advanced Parallel Interference
Cancellation
1: for l = 1,...,L {
2:  for p = P − M_l,...,P {
     for k = 1,...,L {
      if (k ≠ l AND (p)DS(l) = false) {
       Perform interference subtraction of
       packet k in transmission [jp]r as
       shown in Fig. 3.
      }
     }
   }
   After step 2, M_l soft values,
   (m_l)θ(l), m_l = 1,...,M_l, are obtained for
   each code bit.
3: Combine the soft values as Σ_{u=1}^{M_l} (u)θ(l) and
   perform soft decoding.
4: if (CRC check of packet l is OK) {
    Ideally remove the interference of packet
    l from the transmissions [jp]r, p=P−M_l,...,P
    as shown in Fig. 4.
    j_p := j_p + 1
    (p)DS(l) := true
   }
}
5: for p = 1,...,P {
    if (j_p = L) {
    Remove values [L]r and (p)H from the
    buffers of received and fading values,
    respectively
   }
}
6: if (any packet has been decoded in
   steps 1–5) {
   go to 1
}
else end of algorithm
```

The proposed APIC algorithm is summarized in Algorithm 1. As shown in the table, this algorithm is carried out in multiple iterations. A single iteration can be described by steps 1–5.

Up to L packets can be decoded in one iteration. If any packet has been decoded in the iteration, the next iteration starts from step 1, since ideal interference removal can improve the decoding probability of undecoded packets.

If no additional packets can be decoded in the iteration, the algorithm stops and notifies the transmitter about the current decoding status of each transmitted packet. If the packet cannot be decoded, a "NACK," otherwise an "ACK" is generated.

If index j_p, $p = 1, \ldots, P$ reaches the maximum value L, all packets are decoded in ${}^{[L]}\mathbf{r}$. Thus, ${}^{[L]}\mathbf{r}$ contains no more useful information (step 5). The vector ${}^{[L]}\mathbf{r}$ and the corresponding matrix ${}^{(p)}\mathbf{H}$ are removed from the buffer of the received values and from the buffer of the fading values, respectively.

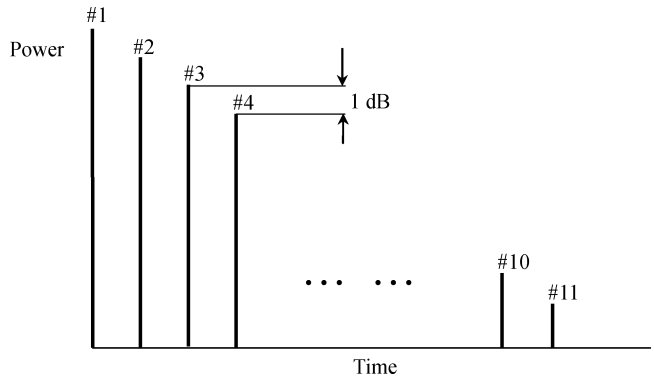

Fig. 5. Delay power profile of time-domain multipath channel model.

IV. Simulation Results

The transmission system under investigation has a bandwidth of $BW = 50$ MHz and the carrier frequency is located at 5 GHz. The total number of subcarriers is $N_c = 1024$. The resulting subcarrier spacing is 48.82 kHz and the OFDMA-CDM symbol duration is 20.4 μs. The modulation is either QPSK, 16-QAM, or 64-QAM. The number of simultaneously active users is 8 and the number of groups is $Q = 16$. WH codes of length $L = 8$ are applied, which is a good compromise between complexity and performance. A convolutional channel encoder with code rate $R = 1/2$ and memory $m_e = 6$ is used for the simulations. Two different channel models are considered in our simulations. The first one is an independent Rayleigh-fading channel model. In this model, Rayleigh fading is assumed to be independent between adjacent subcarriers and OFDMA-CDM symbols [17]. The second model is a time-domain multipath channel model, which consists of a tapped delay line with 11 statistically independent Rayleigh-fading taps. The delay spread is smaller than the guard interval length. The average power for each channel tap is decreasing by 1 dB in comparison with the preceding channel tap, as shown in Fig. 5. Tap #1 has an average power equal 0 dB. Additionally, the average channel attenuation is normalized to unity in our simulation. The speed of a mobile is chosen to be 200 km/h, which represents an application with high mobility.

The performance of a conventional OFDMA system with comparable parameter setting as for OFDMA-CDM is used as a reference. The system parameters for such an OFDMA system are summarized in Table I. OFDMA is employed together with H-ARQ based on MRC. We utilize several subsequent OFDMA symbols for the transmission of the information of one packet. The number of subsequent symbols is 8 for QPSK and 16-QAM, and 4 for 64-QAM.

As another performance reference, an OFDMA-CDM system is used where several subsequent OFDMA-CDM symbols are employed for the transmission of data symbols of one packet. In this case, all spreading codes are assigned for the transmission of one packet. The number of subsequent symbols is 8 for the QPSK and 16-QAM and 4 for 64-QAM. This allocation allows to exploit H-ARQ based on MRC, since in each retransmission the same data symbols are transmitted. In H-ARQ based on MRC, the combination of transmitted chips is performed according to the MRC principle instead of combining

TABLE I
PARAMETERS OF THE DIFFERENT SIMULATION SYSTEMS

	OFDMA-CDM, APIC	OFDMA-CDM, PIC+SVC	OFDMA-CDM, MRC+PIC	OFDMA
Spreading Length, L	8	8	8	1
Number of groups, Q	16	16	16	16
Packet size (QPSK)	2042	2042	2042	2042
Packet size (16QAM)	4090	4090	4090	4090
Packet size (64QAM)	3066	3066	3066	3066
Packet combination type	SVC	SVC	MRC	MRC
Packet allocation type	superimposed. (each packet is associated with one spreading code)	superimposed. (each packet is associated with one spreading code)	several subsequent OFDMA-CDM symbols are employed for data transmismission of one packet	several subsequent OFDMA symbols are employed for data transmismission of one packet
Type of interference cancellation	APIC	PIC	PIC	-

the transmitted bits like in SVC. Therefore, the SNR ratio of the maximum ratio combined signal is increasing with each retransmission. As data detection and decoding technique, soft PIC is applied.

For all considered systems, transmitted packets have the same size of 2042, 4090, and 3066 bits for QPSK, 16-QAM, and 64-QAM, respectively. The number of OFDMA-CDM symbols in the frame $N_{\rm fr}$ is equal to 128 for QPSK and 16-QAM, and 64 for 64QAM.

The maximum achievable data rates depend on the symbol mapping alphabet and are equal to 6.25 Mb/s/user for QPSK, 12.5 Mb/s/user for 16-QAM, and 18.78 Mb/s/user for 64-QAM.

We evaluate the system performance as a function of normalized throughput $T_{\rm thr}$ versus SNR. The normalized throughput is defined as the reciprocal value of the average number of transmissions needed to successfully decode the transmitted packet. Another figure of merit is spectral efficiency. The spectral efficiency is proportional to the normalized throughput and can be defined as the ratio of the instantaneous data rate to the available bandwidth.

The SNR corresponding to $T_{\rm thr} = 0.95$ is referred as the working point in the following. In the simulations, if it is not specified explicitly, we assume $N_{\rm tr} = 10$.

A guard interval greater than the maximum channel delay is appended, and the receiver has perfect channel state information and is perfectly synchronized.

In Fig. 6 the normalized throughput as a function of the SNR is depicted. The modulation alphabet is QPSK. One can see that OFDMA-CDM with APIC performs better than any other technique. At the working point of OFDMA-CDM with APIC, the gain in throughput and bandwidth efficiency is 17.2% compared to OFDMA-CDM with PIC and H-ARQ based on SVC. The bandwidth efficiency gap between OFDMA-CDM with APIC and OFDMA is around 45.2%. The OFDMA-CDM with H-ARQ based on MRC performs 27.1% worse than OFDMA-CDM with APIC. At lower SNR, the performance of APIC is comparable to OFDMA with H-ARQ based on MRC and OFDMA-CDM with H-ARQ based on SVC. OFDMA-CDM outperforms OFDMA at high SNR because spreading exploits the potential frequency diversity. At SNR values lower than 3 dB, the soft PIC cannot cope with SI and OFDMA-CDM performs as conventional OFDMA.

The combination of soft PIC and SVC performs better than a combination of soft PIC and MRC for OFDMA-CDM. This

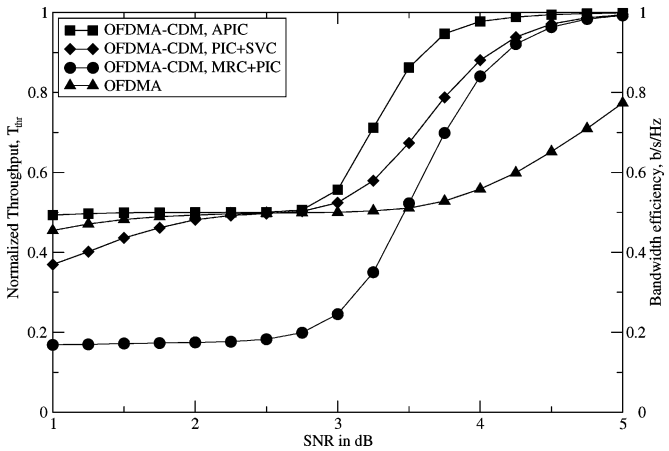

Fig. 6. Normalized throughput for different systems and different H-ARQ schemes versus SNR; QPSK modulation, independent Rayleigh-fading channel.

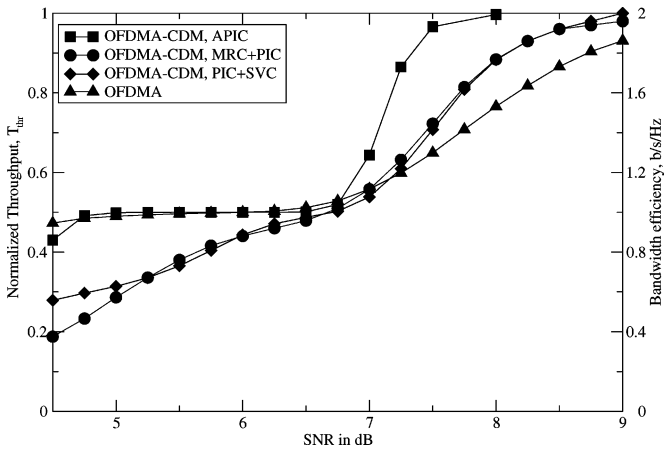

Fig. 7. Normalized throughput for different systems and different H-ARQ schemes versus SNR; 16-QAM modulation, independent Rayleigh-fading channel.

effect can be explained as follows. In H-ARQ based on MRC, the SNR is enhanced in every retransmission, whereas H-ARQ based on SVC exploits a stronger code, and thus, the quality of soft PIC cancellation improves.

In Fig. 7, the modulation is increased to 16-QAM. Again, it can be observed that the OFDMA-CDM scheme with APIC outperforms all other techniques. At the working

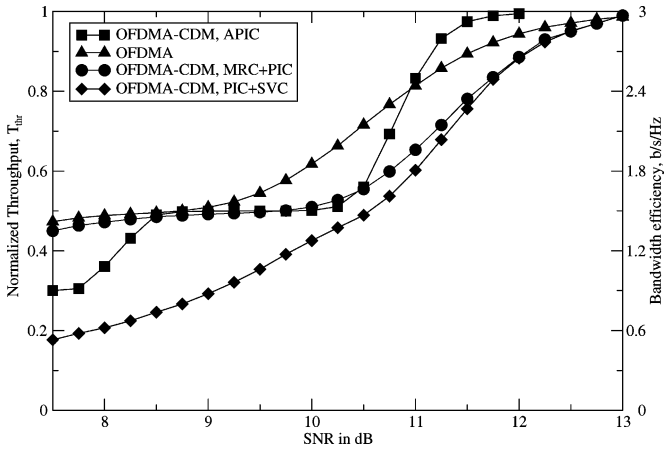

Fig. 8. Normalized throughput for different systems and different H-ARQ schemes versus SNR; 64-QAM modulation, independent Rayleigh-fading channel.

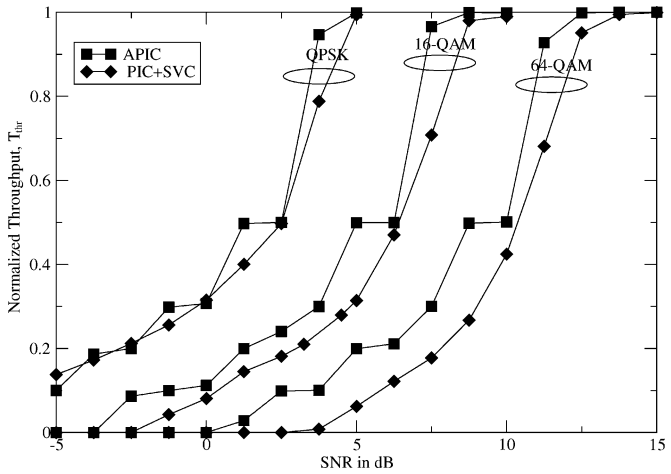

Fig. 9. Normalized throughput for OFDMA-CDM with APIC and OFDMA-CDM with PIC and H-ARQ based on SVC versus SNR; independent Rayleigh-fading channel.

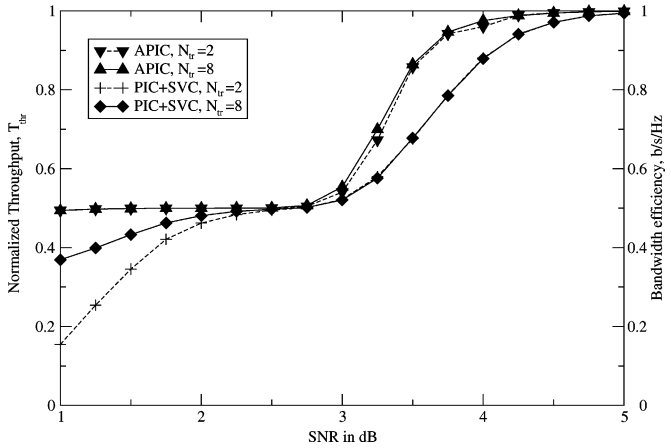

Fig. 10. Normalized throughput for OFDMA-CDM with APIC and OFDMA-CDM with PIC and H-ARQ based on SVC versus SNR for different values of $N_{\rm tr}$; independent Rayleigh-fading channel.

point, the gain in bandwidth efficiency is 26% in comparison with OFDMA-CDM and H-ARQ based on SVC. The OFDMA-CDM system outperforms OFDMA since the soft PIC is still able to combat SI and the OFDMA-CDM system benefits from frequency diversity.

The H-ARQ schemes based on SVC and MRC do not show any difference in the performance for OFDMA-CDM. However, at lower SNR, H-ARQ based on MRC performs better, since the number of retransmissions is large and, thus, MRC is able to combine packets optimally. Nevertheless, at lower SNR, APIC performs better than both MRC and SVC and achieves the performance of OFDMA.

In Fig. 8, the modulation cardinality is further increased to 64-QAM, which leads to increased SI. Therefore, the OFDMA system outperforms OFDMA-CDM with H-ARQ based on SVC and OFDMA-CDM with H-ARQ based on MRC. The explanation of this effect has been given in [19]. In an OFDMA-CDM system, high level of interference dominates over the effect of achieved frequency diversity. Due to the high level of SI, the performance of the OFDMA-CDM system cannot be further improved even with soft PIC. Again, the OFDMA-CDM system with APIC successfully combats SI and outperforms OFDMA at the working point. At high SNR, the SI is the dominant effect which influences the performance. With the iterative algorithm, the decoded packets can be removed ideally which improves the decoding probability of the other packets in the subsequent iterations.

The analysis of the obtained results demonstrate, that neither OFDMA-CDM with H-ARQ based on SVC nor H-ARQ based on MRC nor OFDMA with H-ARQ based on MRC can be chosen as a dominant scheme, since their performances depend on the modulation alphabet. With APIC, an OFDMA-CDM system with adaptive modulation can handle all symbol mapping schemes from QSPK to 64-QAM to increase the data rate so that the multiplexing scheme needs not to be changed to conventional OFDMA to guarantee optimum performance. However, H-ARQ based on MRC provides an optimal performance if the number of retransmissions is large. In this case, all chips of a (re)transmitted packet have nearly the same fading statistics. Therefore, different chips of such a packet are faded equally, and therefore the SI disappears. Additionally, MRC combines chips in the most favorable way to increase the SNR with each retransmission. As a result, H-ARQ based on MRC provides an optimal performance if the number of retransmissions is large.

At lower SNR, the effect of the combination of re-encoded values plays the dominant role. This is clearly visible in Fig. 9. At $T_{\rm thr} = 0.2$, the energy gain provided by APIC comprises 2.5 dB for 64-QAM and about 2 dB for 16-QAM in comparison with conventional H-ARQ based on SVC.

The influence of the maximum allowed number of transmission $N_{\rm tr}$ on the normalized throughput is illustrated in Fig. 10. Two cases with $N_{\rm tr} = 8$ and $N_{\rm tr} = 2$ are considered. The simulation results are presented for OFDMA-CDM with APIC and OFDMA-CDM with PIC and H-ARQ based on SVC. If $N_{\rm tr} = 2$, the combination of PIC and H-ARQ based on SVC degrades rapidly at low SNR. The effective code rate $R = 1/4$ obtained after SVC does not offer high performance at low SNR. Contrary to the simple SVC, the performance of APIC remains

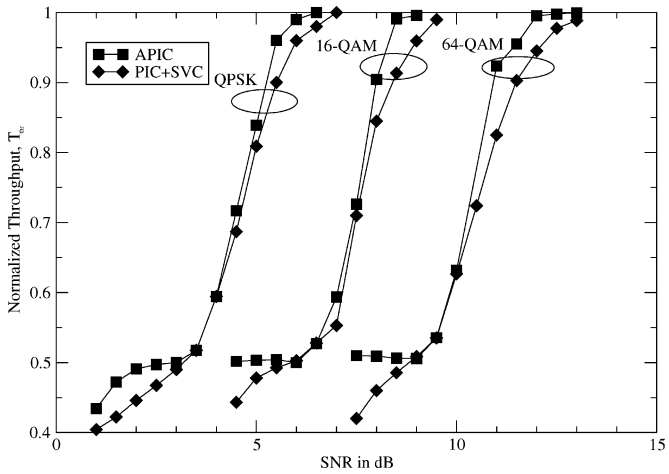

Fig. 11. Normalized throughput for OFDMA-CDM with APIC and OFDMA-CDM with PIC and H-ARQ based on SVC versus SNR; time-domain multipath channel model.

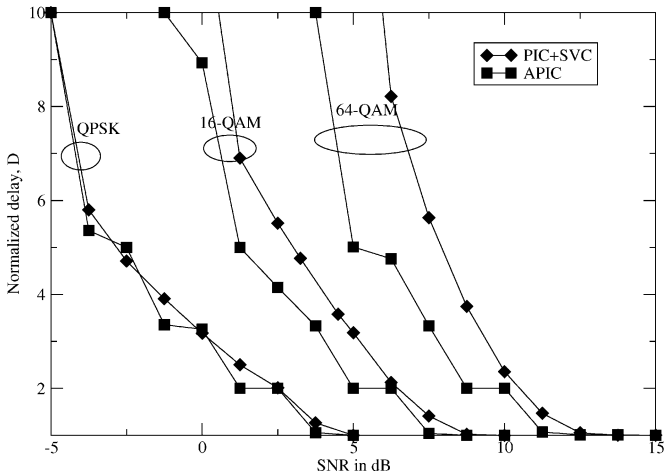

Fig. 12. Normalized delay for OFDMA-CDM with APIC and OFDMA-CDM with PIC and H-ARQ based on SVC versus SNR; independent Rayleigh-fading channel.

constant, even if N_{tr} is small. With the APIC, less retransmission are necessary in order to provide the same performance as with the other H-ARQ techniques.

In Fig. 11, simulation results for the time-domain multipath channel are given. In this channel model, the fading coefficient between adjacent subcarriers and different transmitted frames are correlated. Generally, the greater the correlation in frequency or in time direction, the lower the SI of the received signal. As a consequence, the performance improvement of the soft PIC in the OFDMA-CDM system versus the pure OFDMA system is smaller. However, the reduced potential diversity of this channel results in a lower system performance. Moreover, the Viterbi decoder is not well suited to recover the resulting correlated errors. Fig. 11 shows the APIC is still able to outperform a combination of soft PIC and H-ARQ based on SVC.

One parameter which is important for time critical applications is the latency that occurs during the transmission. In order to compare different techniques, a normalized delay D is introduced. The normalized delay is defined as the average time needed for error-free transmission of a packet, normalized to the frame duration. The normalized delay as a function of SNR is depicted in Fig. 12. The modulation is again a parameter. One can see that the APIC algorithm provides a lower normalized delay, compared with conventional H-ARQ based on SVC. The normalized delay is reduced up to 46% for the 64-QAM at 8.75 dB and up to 24% for 16-QAM at 2.5 dB.

One can see from Fig. 9 that the normalized throughput curves for the APIC algorithm have a stepwise characteristic. In flat areas, the algorithm is able to provide a constant performance, even with decreasing SNR. The explanation of this effect is reflected in Fig. 13. In this figure, the percentage of the packets decoded in different iterations is shown for the case of QPSK. This percentage is calculated as follows. We generate L packets of data, transmit them, and try to decode them by applying the APIC algorithm. Then, we measure the number of packets decoded in different iterations. In this process, each packet can be retransmitted several times. At an SNR lower than 2 dB, the data packets cannot always be decoded in a

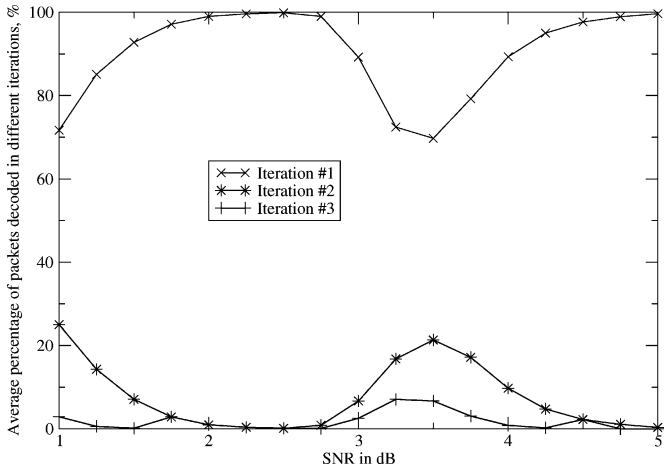

Fig. 13. The percentage of packets decoded in different iterations for OFDMA-CDM with APIC and using QPSK modulation; independent Rayleigh-fading channel.

single iteration. The constant performance is mainly provided by the second and the third iteration. This is similar between 3–4 dB, where more iterations for interference cancellation improve the performance and avoid retransmissions. Between 2–3 dB more iterations of the APIC does not improve the performance. Therefore, more retransmissions are needed to be able to decode all packets of the frame. Our simulations show that typically three iterations are enough, and further iterations do not improve the performance significantly.

The complexity of the proposed system can be addressed as follows. The main part of the complexity of the APIC is concentrated in the soft in/soft out channel decoder. The calculation of the re-encoded values needs to be performed only once per each retransmission per packet. The subsequent manipulations are simply the combination of already obtained re-encoded values. Thus, the complexity of the proposed scheme grows only linearly with the number of retransmissions.

It can be summarized that at higher SNR, where the number of overall transmissions is small, the dominant effect in the APIC performance is ruled by ideal interference cancellation. In this

case, the interference caused by decoded packets can be perfectly reconstructed and subtracted.

V. Conclusion

Superimposed packet allocation for OFDMA-CDM transmission has been proposed. An iterative APIC algorithm, which is a combination between H-ARQ based on SVC and PIC has been presented. The simulation results show that the proposed algorithm outperforms an OFDMA system with H-ARQ based on SVC, an OFDMA-CDM system with PIC and H-ARQ based on SVC, and an OFDMA-CDM system with H-ARQ based on MRC and PIC. The reason for this is that OFDMA-CDM with APIC successfully exploits the frequency diversity provided by the CDM component and at the same time combats SI more efficiently. The ideal interference cancellation scheme allows the receiver to remove the interference at high SNR, where the packet error rate does not exceed 5%. The advantages of re-encoded values combining appear especially at lower SNR, where the number of retransmissions is large. Thus, the proposed algorithm is an interesting technique for future wireless high data rate transmission systems.

Acknowledgment

The authors would like to acknowledge the support and opportunity to conduct this research work.

References

[1] K. Fazel and S. Kaiser, *Multi-Carrier and Spread Spectrum Systems*, West Sussex, U.K.: Wiley, 2003.

[2] S. Kaiser, "OFDM code-division multiplexing in fading channels," *IEEE Trans. Commun.*, vol. 50, no. 8, pp. 1266–1273, Aug. 2002.

[3] S. Kaiser and J. Hagenauer, "Multi-carrier CDMA with iterative decoding and soft-interference cancellation," in *Proc. IEEE Global Telecommun. Conf.*, Nov. 1997, pp. 6–10.

[4] G. Berrou and A. Glavieux, "Near optimum error correcting coding and decoding: Turbo codes," *IEEE Trans. Commun.*, vol. 44, pp. 1261–1271, Oct. 1996.

[5] X. Wang and H. V. Poor, "Iterative (turbo) soft interference cancellation and decoding for coded CDMA," *IEEE Trans. Commun.*, vol. 47, no. 7, pp. 1046–1061, Jul. 1999.

[6] S. Wicker, *Error Control Systems for Digital Communications and Storage*. Englewood Cliffs, NJ: Prentice-Hall, 1995.

[7] J. Hagenauer, "Rate compatible punctured convolutional codes (RCPC codes) and their application," *IEEE Trans. Commun.*, vol. 36, pp. 389–400, Apr. 1988.

[8] D. Chase, "Code combining–A maximum-likelihood decoding approach for combining an arbitrary number of noisy packets," *IEEE Trans. Commun.*, vol. COM-33, no. 5, pp. 385–393, May 1985.

[9] H. Atarashi, S. Abeta, and M. Sawahashi, "Performance evaluation of coherent high-speed TD-OFCDM broadband packet wireless access in forward link employing multi-level modulation and hybrid ARQ," *IEICE Trans. Fundamentals*, vol. E84-A, no. 7, pp. 1670–1680, Jul. 2001.

[10] N. Miki, S. Abeta, and M. Sawahashi, "Evaluation of throughput employing hybrid ARQ packet combining in forward link OFCDM broadband wireless access," in *Proc. 13th IEEE Int. Symp. Pers., Ind., Mobile Commun.*, vol. E84-A, Lisboa, Portugal, Sep. 2002, pp. 394–398.

[11] P. Frenger, S. Parkvall, and E. Dahlman, "Performance comparison of HARQ with Chase combining and incremental redundancy for HSDPA," in *Proc. Veh. Technol. Conf.*, Rhodos, Greece, May 2001, pp. 1829–1833.

[12] J. Cheng, "On the coding gain of incremental redundancy over Chase combining," in *Proc. IEEE Global Telecommun. Conf.*, San Francisco, CA, Dec. 2001, pp. 107–112.

[13] M. Gidlund and P. Åhag, "Enhanced HARQ scheme based on rearrangement of signal constellations and frequency diversity for OFDM systems," in *Proc. IEEE Veh. Technol. Conf.-Spring*, Milan, Italy, May 2004, pp. 500–504.

[14] T. Kumagi, M. Mizoguchi, T. Onizawa, H. Takanashi, and M. Morikura, "A maximal ratio combining frequency diversity ARQ scheme for OFDM signals," in *Proc. 9th. IEEE Int. Symp. Pers., Ind., Mobile Commun.*, vol. 2, Boston, MA, May 2001, pp. 528–532.

[15] C. Wengerter, A. V. Elbart, E. Seidel, G. Velev, and M. Schmitt, "Advanced hybrid ARQ technique employing a signal constellation rearrangement," in *Proc. IEEE Veh. Technol. Conf.-Fall*, Vancouver, BC, Canada, Sep. 2002.

[16] V. Kawadia and P. Kumar, "A cautionary perspective on cross-layer design," *IEEE Wireless Commun.*, vol. 12, no. 1, pp. 3–11, Feb. 2005.

[17] J. Proakis, *Digital Communications*, 4th ed. New York: McGraw-Hill, 2001.

[18] J. Hagenauer, "Forward error correcting for CDMA systems," in *Proc. IEEE 4th Int. Symp. Spread Spectrum Tech. Appl.*, Sep. 1996, pp. 566–569.

[19] R. Raulefs, A. Dammann, S. Kaiser, and G. Auer, "Comparing multicarrier based broadband systems for higher modulation cardinalities," in *Proc. Veh. Technol. Conf.-Fall*, Los Angeles, CA, Sep. 2004.

[20] IST. 4MORE Project. [Online]. Available: http://www.ist-4more.org

Alexander Arkhipov received the M.Sc. degree in electrical engineering from the Moscow State Engineers and Physics Institute, Moscow, Russia, in 1998 and the M.Sc. degree in communications engineering from the University of Ulm, Ulm, Germany, in 2001. Currently, he is working towards the Ph.D. degree in electrical engineering at the German Aerospace Center (DLR), Institute of Communications and Navigation, Wessling, Germany.

His research interests include digital communications with an emphasis on spread-spectrum and multicarrier systems, coding, and preequalization techniques.

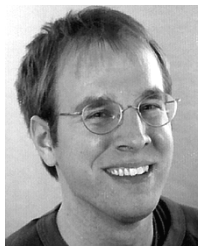

Ronald Raulefs studied electrical engineering at the University of Kaiserslautern, Kaiserslautern, Germany. From November 1997 to June 1998, he was at the University of Edinburgh, Scotland, as an Erasmus student. He received the Dipl.-Ing. degree from the University of Kaiserslautern, in 1999.

Since 1999, he has been a Researcher at the German Aerospace Center (DLR), Institute of Communications and Navigation, Wessling, Germany. His main research interests focus on MIMO systems, iterative detection techniques and joint-layer optimizations for cellular mobile radio systems.

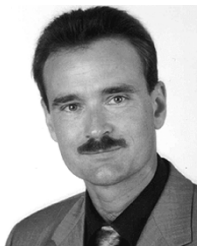

Michael Schnell (M'96–SM'04) received the Dipl.-Ing. degree in electrical engineering from University of Erlangen-Nuremberg, Germany, in 1989, and the Ph.D. from the University of Essen, Essen, Germany, in 1997.

In 1990, he joined the German Aerospace Center (DLR), Institute of Communications and Navigation, Wessling, Germany. From October to December 1997, he was a Visiting Researcher with the University of Victoria, BC, Canada. Since 1999, he is Leader of the Aeronautical Communications and Multiple-Access Group at the Institute of Communications and Navigation of DLR. His main research interests comprise multicarrier communications, multiple-access schemes, diversity techniques, and cognitive radio for aeronautical and terrestrial wireless applications.

Dr. Schnell is a Lecturer for multicarrier communications at the University of Karlsruhe, Karlsruhe, Germany. He is member of the Organizing Committee of the IT Society of the IEEE Germany Chapter and a member of the VDE/ITG.